Structure characterizations and protein resistance of chitosan membranes selectively crosslinked by poly(ethylene glycol) dimethacrylate

Chia-Chu Cheng, Fwu-Long Mi, Shan-hui Hsu & Trong-Ming Don

Cellulose

ISSN 0969-0239
Volume 21
Number 3

Cellulose (2014) 21:1431-1444
DOI 10.1007/s10570-014-0231-5

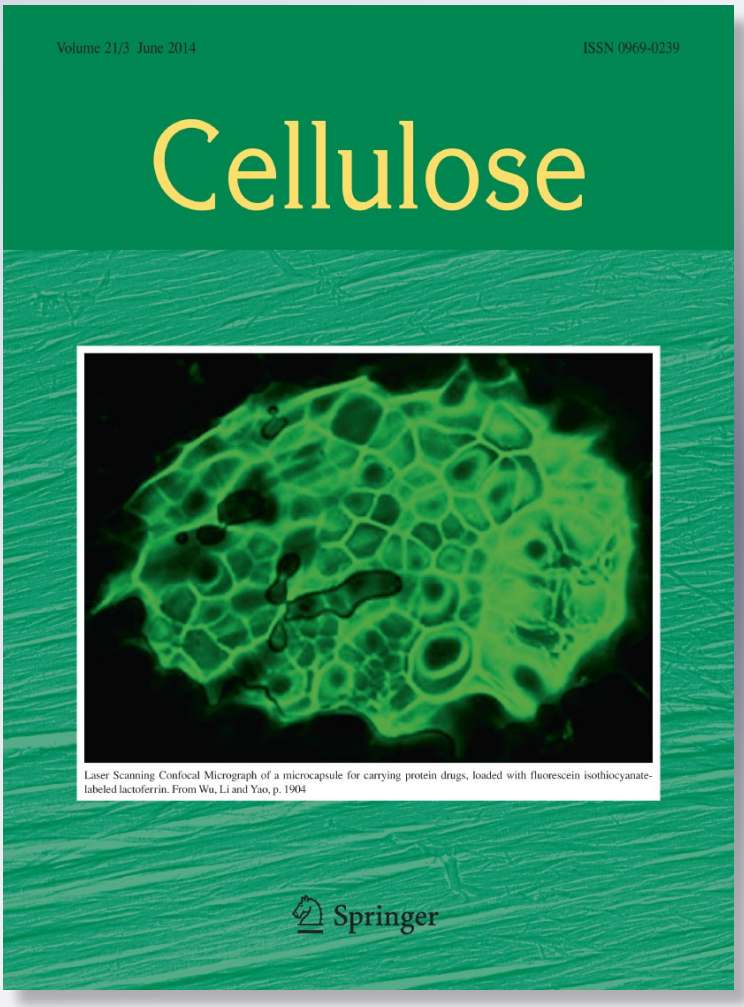

Springer

Cellulose (2014) 21:1431–1444
DOI 10.1007/s10570-014-0231-5

ORIGINAL PAPER

Structure characterizations and protein resistance of chitosan membranes selectively crosslinked by poly(ethylene glycol) dimethacrylate

Chia-Chu Cheng · Fwu-Long Mi · Shan-hui Hsu · Trong-Ming Don

Received: 6 November 2013 / Accepted: 4 March 2014 / Published online: 8 March 2014

Abstract Chitosan (CS) is a fragile material with a high modulus of elasticity. Improving its flexibility as well as membrane permeability are the key aspects that need to be addressed for using CS as a biomaterial. Poly(ethylene glycol) (PEG) has several unique properties such as protein resistance, low toxicity, immunogenicity, and good solubility in both water and organic solvents. In this study, a vinyl compound was grafted to the C-6 position of CS by protection-grafting-deprotection. The vinyl CS was then crosslinked with PEG dimethacrylate (PEGDMA) selectively at its C-6 position to form CS-*g*-PEG copolymer membranes. Analyses from spectra of Fourier-transform infrared and nuclear magnetic resonance confirmed the chemical structure of the crosslinking CS-*g*-PEG copolymer membranes. Thermal and mechanical properties of the prepared CS-*g*-PEG membranes were measured and well-correlated to their structures. The incorporation of PEGDMA into the CS increased the material's flexibility and thermal resistance. Finally, the CS-*g*-PEG membranes were found to have good protein resistance and blood compatibility; therefore, it has potential application as the biomedical material especially for hemodialysis.

Keywords Chitosan · Poly(ethylene glycol) dimethacrylate · Copolymer membrane · Protein resistance

Electronic supplementary material The online version of this article (doi:10.1007/s10570-014-0231-5) contains supplementary material, which is available to authorized users.

C.-C. Cheng · T.-M. Don (✉)
Department of Chemical and Materials Engineering, Tamkang University, Tamsui District, New Taipei City 25137, Taiwan
e-mail: tmdon@mail.tku.edu.tw

F.-L. Mi
Department of Biochemistry, School of Medicine, Taipei Medical University, Taipei 110, Taiwan

F.-L. Mi
Graduate Institute of Medical Sciences, College of Medicine, Taipei Medical University, Taipei 110, Taiwan

S. Hsu
Institute of Polymer Science and Engineering, National Taiwan University, Taipei, Taiwan

Introduction

Chitosan (CS) is a linear polysaccharide composed mainly of β-1,4-glucosamine and partly of β-1,4-*N*-acetyl glucosamine, and is generally obtained via the deacetylation of chitin in a hot strong concentrated alkali solution. It can be dissolved in an acid solution and becomes a cationic polymer because of the protonation of amino group at C-2 position of pyranose ring. CS has been used in a lot of fields such as in the food industry, cosmetics, pharmaceuticals, nutrition and environmental pollution control. Especially for its advantages in wound healing such as

hemostasis, accelerating the tissue regeneration and the fibroblast synthesis of collagen, many applications of CS in skin tissue engineering have been reported (Harish Prashanth and Tharanathan 2007; Rinaudo 2006). However, CS is a fragile material with a high modulus of elasticity, because of its strong hydrogen bonding and high crystallinity. Improving its flexibility as well as membrane permeability are the key aspects that need to be addressed for using CS as a biomaterial. Blending or copolymerization with synthetic flexible polymers may be the good way for improving its properties. Several synthetic polymers have been selected to be blended with CS, but the biocompatible and hydrophilic poly(ethylene glycol) (PEG) is of particular interest. This is because PEG has several unique properties such as protein resistance, low toxicity, immunogenicity, and good solubility in both water and organic solvents. It has no negative effects on protein conformation and shows good ability to protect the activities of enzymes (Colonna et al. 2008). In addition, PEG is one of the few synthetic polymers that have been approved for the use in food, cosmetics, personal care products, and pharmaceutical. Because of the good biological activities of CS and PEG, a combination of both may have beneficial effects on the biological properties of the prepared complex membranes. Therefore, PEG has been applied for improving biocompatibility and hydrophilicity of many materials mostly by chemical modification, i.e. PEGylation. Peng et al. (2010) synthesized a CS-*g*-PEG graft copolymer in an attempt to increase the water solubility. Bhattarai et al. (2005) prepared a CS-*g*-PEG injectable thermogel by alkylation of CS via Schiff-base reaction with a PEG-aldehyde. Mao et al. (2005) investigated the uptake and transport mechanisms of insulin in the nanocomplexes formed by the self-assembly of PEGylated trimethyl CS copolymer with particle size between 200 and 400 nm. Lin and Chen (2007) prepared CS-*g*-PEG-galactose having sufficient amount of targeting moieties for asialoglycoprotein receptor on hepatocytes. Li et al. (2009) synthesized hydrogels based on water-soluble CS-ethylene glycol acrylate methacrylate (CS-EGAMA) and polyethylene glycol dimethacrylate (PEGDMA). However, most PEGylations of CS are through the reaction with the amino group, which, especially with high degree of substitution, would change the fundamental skeleton of CS and lose its original physicochemical and biological activities. Therefore, modification of CS through hydroxyl groups may have an advantage that the free amino groups can be retained and biological activities can thus be preserved. Don and Chen (2005) grafted a thermo-responsive polymer, poly(*N*-isopropyl acrylamide) (PNIPAAm), to CS at the C-2 position (amino group) and the resulting CS-*g*-PNIPAAm copolymer membrane had a poor cellular viability (L929 cells). However, if the amino groups were preserved by grafting the PNIPAAm at the C-6 position (hydroxyl group), the cellular compatibility of the CS-*g*-PNIPAAm membrane was as good as the pure CS, as long as the grafting ratio of PNIPAAm was below 1.7 (Don et al. 2011). Unfortunately, amino group is generally more chemically active than hydroxyl group. Therefore, the modification through hydroxyl group requires more elaborate reactions.

In this study, a crosslinking CS-*g*-PEG copolymer membrane was prepared by reacting poly(ethylene glycol) dimethacrylate (PEGDMA) selectively at the C-6 position of CS. For achieving this goal, a vinyl functional group was endowed to the CS at its C-6 position as the crosslinking site via a protection-grafting-deprotection procedure. To protect the more active amino groups at C-2 position, CS was reacted with phthalic anhydride (PA) to form phthaloylated CS (PACS) in a formic acid/DMF solution. A vinyl compound was then grafted to the PACS, preferentially with the hydroxyl group at C-6 position. The phthaloyl groups were subsequently removed by hydrazine to recover all the amino groups in CS. Finally, the vinyl CS was crosslinked with PEGDMA through the vinyl groups at C-6 position by a UV-initiated free-radical polymerization to form a crosslinking CS-*g*-PEG copolymer membrane. The detailed reactions are shown in Fig. 1. FTIR and NMR were used to analyze the chemical structure of CS-*g*-PEG membrane. In addition to the thermal and mechanical properties, protein resistance and blood compatibility of CS-*g*-PEG copolymer membranes were all evaluated.

Experimental

Materials

Chitosan was obtained from Tokyo Chemical Inc. (Tokyo, Japan). Because of its high viscosity in the acid solution which was not favorable for the chemical

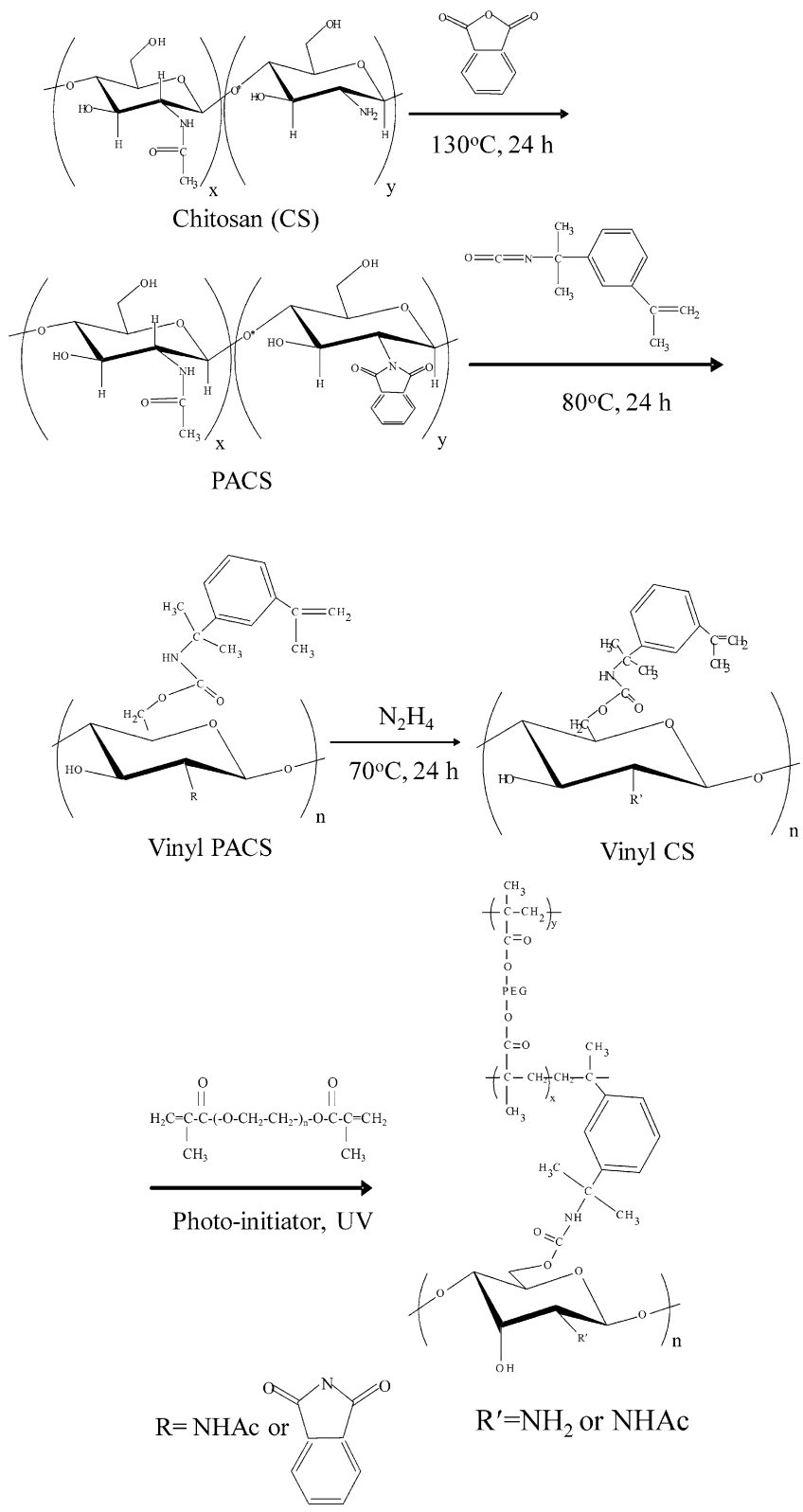

Fig. 1 Synthetic route and proposed structure of the selectively crosslinked CS-*g*-PEG graft copolymer membranes

modification, CS was purified and degraded in an acetic acid solution (1 wt%) at 80 °C for 24 h before use. The degraded CS had a viscosity average molecular weight of 96 kDa determined by a viscometric method and the Mark–Houwink equation (Don and Chen 2005). Nuclear magnetic resonance (NMR) was used to determine the values of the degree of deacetylation (DDA, equivalent to the moles of amino group per mole of pyranose ring) of CS (Lavertu et al. 2003). Both DDA values before and after degradation were found to be the same at 85.0 %. Phthalic anhydride (PA) was obtained from Showa (Tokyo, Japan). Poly(ethylene glycol) dimethacrylate (PEGDMA, 550 g mol^{-1}), dibutyltin dilaurate, 3-isopropenyl-$\alpha\alpha'$-dimethylbenzyl isocyanate (IPDI), β-glucosidase (5.2 unit mg^{-1}), and *p*-nitrophenyl-β-D-glucopyranoside were all purchased from Sigma (St. Louis, MO, USA). Hydrazine hydrate (80 % in H_2O) was obtained from Riedel-de Haën (Hannover, Germany). The photo-initiator, 2-hydroxy-2-methylphenyl-1-propanone (HMPP), also called "Darocure 1173", was purchased from Merck (Darmstadt, Germany). Other chemical reagents are at least reagent grade and used without further purification.

Synthesis of vinyl chitosan and CS-*g*-PEG membranes

In order to crosslink CS selectively at its C-6 position by PEGDMA, a series of protection-grafting-deprotection was carried out to endow the CS with vinyl functional group at its C-6 position. The amino group at C-2 position of CS was first protected by reaction with PA to form a phthaloylated CS (PACS); and a vinyl compound was then grafted to the PACS preferentially at C-6 position through the urethane linkage to provide the reactive site for further crosslinking. The phthaloyl groups were finally removed by hydrazine to recover all the amino groups in CS. The reactions of protection-grafting-deprotection were similar to those described in our previous paper (Don et al. 2011). Briefly, CS (3.00 g, 0.015 mol of amino group) was dissolved in pure formic acid. After dissolution, it was added with the PA solution prepared by dissolving 45.0 g (0.304 mol) of PA in DMF. The protection reaction was carried out in a nitrogen atmosphere at 130 °C for 24 h. The resulting pale tan solution was poured into an excess acetone to precipitate the PACS product. To provide the vinyl functional group to CS, the vinyl compound IPDI (24.2 g, 0.12 mol) was grafted to the PACS (5.00 g) dissolved in DMAc under a nitrogen atmosphere and catalyzed by dibutyltin dilaurate (1 wt% of IPDI) at 80 °C for 24 h. The reaction product, vinyl PACS, was precipitated out from the solution by adding five times volume of methanol. The phthaloyl groups in vinyl PACS were removed by reduction using hydrazine in DMF/water solution at 80 °C for 9 h under a nitrogen atmosphere. Finally, the vinyl CS, having both amino and vinyl groups, was obtained by precipitation in acetone as shown in Fig. 1.

For the synthesis of CS-*g*-PEG membranes, the vinyl CS ($W_{vinyl\ CS}$) was dissolved in formic acid at a concentration of 10 % (w/v). The solution was then added with different amounts of PEGDMA (W_{PEGDMA}), followed by adding 2 wt% (based on PEGDMA) of photo initiator (Darocure 1173). The solution was poured in a Teflon mold and pre-baked at 50 °C to reach a solid content about 80–85 %. Crosslinking of CS by PEGDMA was then carried out under UV irradiation at an energy level of 500 mJ cm^{-2}. After reaction, the product was post-cured at 50 °C. The crosslinked CS-*g*-PEG membrane was then removed and immersed in the distilled water for 2 days to remove the un-reacted PEGDMA. Finally, the membrane was freeze-dried by lyophilization at −20 °C and then weighed ($W_{CS\text{-}g\text{-}PEG}$). The detailed reactions are shown in Fig. 1. The conversion (X, %) and grafting ratio (GR) values were determined through the gravimetric method according to the following equations:

$$\begin{aligned} X &= (\text{Weight of the reacted PEGDMA}/\\ &\quad \text{weight of initial PEGDMA}) \times 100\\ &= \left(W_{CS-g-PEG} - W_{vinylCS}\right)/W_{PEGDMA} \times 100 \end{aligned} \quad (1)$$

$$\begin{aligned} GR &= (\text{Weight of the reacted PEGDMA}/\\ &\quad \text{weight of vinyl CS})\\ &= \left(W_{CS-g-PEG} - W_{vinylCS}\right)/W_{VinylCS} \end{aligned} \quad (2)$$

For comparison, a crosslinked X-PEG membrane alone was also synthesized in the same way by UV photo polymerization of PEGDMA.

Structure characterizations

Structure analysis of intermediates and final CS-*g*-PEG membranes was carried out with a Fourier

transform infrared (FTIR) spectrophotometer (model 550, Nicolet). Samples were ground into powder and mixed with KBr powder. The mixture was then pressed into a transparent disc and scanned from 4,000 to 400 cm^{-1} for 32 times with a resolution of 4 cm^{-1}. FTIR data for the CS: 3,423 cm^{-1} (–OH, –NH and $–NH_2$ stretching), 2,921 and 2,875 cm^{-1} (C–H stretching), 1,654 cm^{-1} (amide I, C=O stretching), 1,557 cm^{-1} (amide II, N–H bending), 1,595 cm^{-1} (NH_2 bending), 1,421 and 1,321 cm^{-1} (C–H bending), 1,380 cm^{-1} (C–H bending and C–N stretching), 1,260, 1,153, 1,083 and 1,031 cm^{-1} (C–O stretching). PACS: 3,473 cm^{-1} (–OH and –NH stretching), 3,065, 873 and 720 cm^{-1} (phenyl ring), 2,942 and 2,874 cm^{-1} (C–H stretching), 1,778 and 1,712 (imide, C=O stretching), 1,541 cm^{-1} (amide II, N–H bending), 1,469 and 1,313 cm^{-1} (C–H bending), 1,390 cm^{-1} (C–H bending and C–N stretching), 1,293, 1,154, 1,114 and 1,065 cm^{-1} (C–O stretching), 720 cm^{-1} (phenyl ring). Vinyl CS: 3,403 cm^{-1} (–OH and –NH stretching), 3,084 cm^{-1} (phenyl ring), 2,974, 2,924 and 2,876 cm^{-1} (C–H stretching), 1,718 (urethane, C=O stretching), 1,664 cm^{-1} (amide I, C=O stretching), 1,628 cm^{-1} (C=C stretching), 1,599 cm^{-1} (NH_2 bending), 1,538 cm^{-1} (amide II, N–H bending), 1,457 and 1,311 cm^{-1} (C–H bending), 1,381 cm^{-1} (C–H bending and C–N stretching), 1,258, 1,154 and 1,074 cm^{-1} (C–O stretching). CS-*g*-PEG1 (vinyl CS/PEGDMA = 1/1): 3,365 cm^{-1} (–OH, –NH and $–NH_2$ stretching), 2,933 and 2,872 cm^{-1} (C–H stretching), 1,716 cm^{-1} (C=O stretching), 1,658 cm^{-1} (amide I, C=O stretching), 1,539 cm^{-1} (amide II, N–H bending), 1,453 cm^{-1} (C–H bending), 1,375 cm^{-1} (C–H bending and C–N stretching), 1,253, 1,068 and 1,030 cm^{-1} (C–O stretching).

Chemical structures of various samples were also analyzed by ^1H solution NMR (Bruker AC-300 NMR). Different solvents were used for dissolving different kinds of samples to obtain ^1H-NMR spectra: DCl/D_2O for pure CS, *d*-DMSO for PACS and CD_3COOD/D_2O for vinyl CS. ^1H NMR spectra data for the CS: δ 2.08 ppm (CH_3 of NHAc), 3.21 ppm (H-2 of GlcN residue), 3.50–4.20 ppm (H-2 of *N*-acylated GlcN and H-3, 4, 5, 6 of GlcN unit), 4.73 ppm (H-1 of *N*-acylated GlcN residue), 4.87 ppm (H-1 of GlcN residue). PACS: δ 2.09 ppm (CH_3 of NHAc), 3.20 ppm (H-2 of GlcN residue), 3.50–4.20 ppm (H-2 of *N*-acylated GlcN and H-3, 4, 5, 6 of GlcN unit), 4.98 ppm (H-1 of *N*-acylated GlcN residue), 5.07 ppm (H-1 of GlcN residue), 7.54 and 7.79 ppm (Ph). Vinyl CS: δ 1.66 and 2.20 ppm ($–CH_3$ of IPDI), 2.10 ppm (CH_3 of NHAc), 3.22 ppm (H-2 of GlcN residue), 3.50–4.20 ppm (H-2 of *N*-acylated GlcN and H-3, 4, 5, 6 of GlcN unit), 5.23 and 5.49 ppm ($C=CH_2$), 7.43 and 7.64 ppm (Ph).

Elemental analyses of samples were performed with an elementary analyzer (Elementar vario EL III, Germany) to determine the degree of phthaloylation (DS_{PA}, moles of phthaloyl group per mole of pyranose unit) in PACS, $(C_8H_{13}O_5N)_{0.15}(C_6H_{11}O_4N)_{0.85}(C_8H_{2-}O_2)_x{\cdot}y(H_2O)$, and the degree of addition of vinyl group (DS_{vinyl}, moles of vinyl group per mole of pyranose unit) in vinyl CS, $(C_8H_{13}O_5N)_{0.15}(C_6H_{11}O_4N)_{0.85}(C_{13}H_{15}NO)_x$.

Thermal and mechanical properties

Thermal degradation behavior of various samples was investigated using a thermal gravimetric analyzer (Hi-Res TGA 2950 from TA Instruments). A certain amount of sample (8–12 mg) was placed in a platinum pan and heated to 100 °C, held for 5 min to remove residual moisture, and then heated from 100 to 800 °C at a rate of 20 °C min^{-1} under a nitrogen atmosphere.

Tensile mechanical properties of CS-*g*-PEG membranes were measured using a universal testing machine (Shimadzu, Model AGS-J, Japan). Tensile test specimens were prepared through a die cut based on an ASTM standard D638. The specimens had a thickness of 1 mm and the tensile speed was 0.5 mm min^{-1}. Approximately 5 specimens were tested for each sample and the results were averaged. Dynamic mechanical properties were measured with a DMA instrument Q800 from TA Instruments. Rectangular samples with 40 mm in length and 5 mm in width were tested using the tensile mode. The frequency and the amplitude were set at 1 Hz and 10–15 μm, respectively. The samples were heated from −100 to 220 °C at a heating rate of 3 °C min^{-1}. Storage modulus, loss modulus and loss tangent curves were all recorded during heating.

Water absorption and enzymatic degradability of CS-*g*-PEG membranes

The water absorption was determined by swelling the CS-*g*-PEG membranes which were cut into a circular disc of 2 cm in diameter in the phosphate buffer solutions at various pH values but all at 37 °C. Before

immersion, the membrane was dried in a vacuum oven at 70 °C until a constant weight (W_o) was reached. After immersion for a certain time, the wet membrane was removed and wiped with a lens-cleaning tissue to remove the water on the surface. It was then weighed. The procedure was repeated until there was no further change in the weight. The final weight of the swollen membrane was denoted as W_{eq}. The equilibrium swelling ratio (SR, g/g) was then calculated as $SR = W_{eq}/W_o$.

The pre-dried sample with a diameter of 1.5 cm was weighed (W_o) and then immersed into a phosphate buffer solution (pH 7.4) containing lysozyme at a concentration of 0.5 mg mL^{-1}. It was incubated at 37 °C for a certain period of time. The membrane was then removed, washed with distilled water and dried at 50 °C for 1 day followed by in the vacuum oven at 70 °C for 3 h. The sample was weighed again (W) and the weight loss percentage up to 28 days was thus calculated.

Protein resistance and blood compatibility

Protein resistance was evaluated by immersing various CS-*g*-PEG membranes with a diameter of 1.5 cm into 2 mL β-glucosidase solution with a concentration of 1 mg mL^{-1}. After incubation at 4 °C for 24 h, 0.2 mL of the enzyme solution was drawn out and mixed with 1.8 mL of 5 mM substrate solution which was prepared by dissolving *p*-nitrophenyl-β-D-glucopyranoside in a 0.1 M acetic acid buffer solution. The β-glucosidase could catalyze the hydrolysis of *p*-nitrophenyl-β-D-glucopyranoside to produce *p*-nitrophenol. After 2 min of reaction, 4 mL of 1 M Na_2CO_3 solution was added to stop the reaction. The absorbance at 400 nm (A_{24h}) of the *p*-nitrophenol in the solution was then measured to determine the residual enzyme activity. The original enzyme activity was also determined by the same procedure. Its absorbance at 400 nm was denoted as A_o. The protein resistance was thus defined as A_{24h}/A_o.

Blood compatibility was examined by observing the surface of blood-contacting membranes. The prepared membranes with 1.5 cm in diameter were sterilized with 70 % alcohol and placed in wells of a 24-well tissue culture polystyrene plate (Corning, Action, MA, USA). They were first rinsed with PBS solution and then platelet rich plasma (PRP) with 1 mL (6×10^8–14×10^8 cell/mL) was layered on the sample membranes. They were cultured in a humidified incubator balanced with 5 % CO_2 at 37 °C for 1 h. Subsequently, the membranes were washed with PBS solution to remove the free and physically-adsorbed platelets. They were then treated with 2.0 % glutaraldehyde PBS solution for 5 min and washed with distilled water. Finally, they were dried and sputter-coated with a thin layer of gold for SEM observation.

Results and discussion

Synthesis of CS-*g*-PEG copolymer membranes

In this study, crosslinking CS-*g*-PEG copolymer membranes were prepared by UV-initiated photopolymerization of PEGDMA with the vinyl-functionalized CS. The reasons for choosing crosslinking with PEGDMA instead of grafting polymerization with poly(ethylene glycol) methacrylate (PEGMA) as reported in most papers are described below. First, the prepared CS-*g*-PEG copolymers were intended to be used as membranes for hemodialysis. By grafting PEGMA to CS, the obtained graft copolymer is expected to have a high swelling ratio and even could dissolve in aqueous solution, especially in an acidic environment, because both components are hydrophilic. Radhakumary et al. (2009) reported that the swelling ratio (W_{eq}/W_o) in the pH 7.4 buffer after 1 h reached 2.5 for the branched CS-*g*-PEGMA membrane with a grafting ratio of 1.64, and a value as high as 5.6 was obtained when the grafting ratio was increased to 3.2. This large swelling ratio could compromise the performance of the membrane for hemodialysis. By creating a crosslinking structure, the swelling ratio could be greatly decreased. In addition, the crosslinking extent could be controlled by the added amount of the PEGDMA. Moreover, the membrane with a crosslinking structure would be more resistant to biodegradation which is beneficial for the application in hemodialysis and will be discussed later. Yet, the crosslinking reaction by PEGDMA was designed to occur selectively at the C-6 position of CS to preserve the amino groups at the C-2 position as shown in Fig. 1. Therefore, a series of protection-grafting-deprotection was carried out as described in our previous paper (Don et al. 2011). The more active amino group was first protected by reaction with phthalic anhydride (PA) at 130 °C to

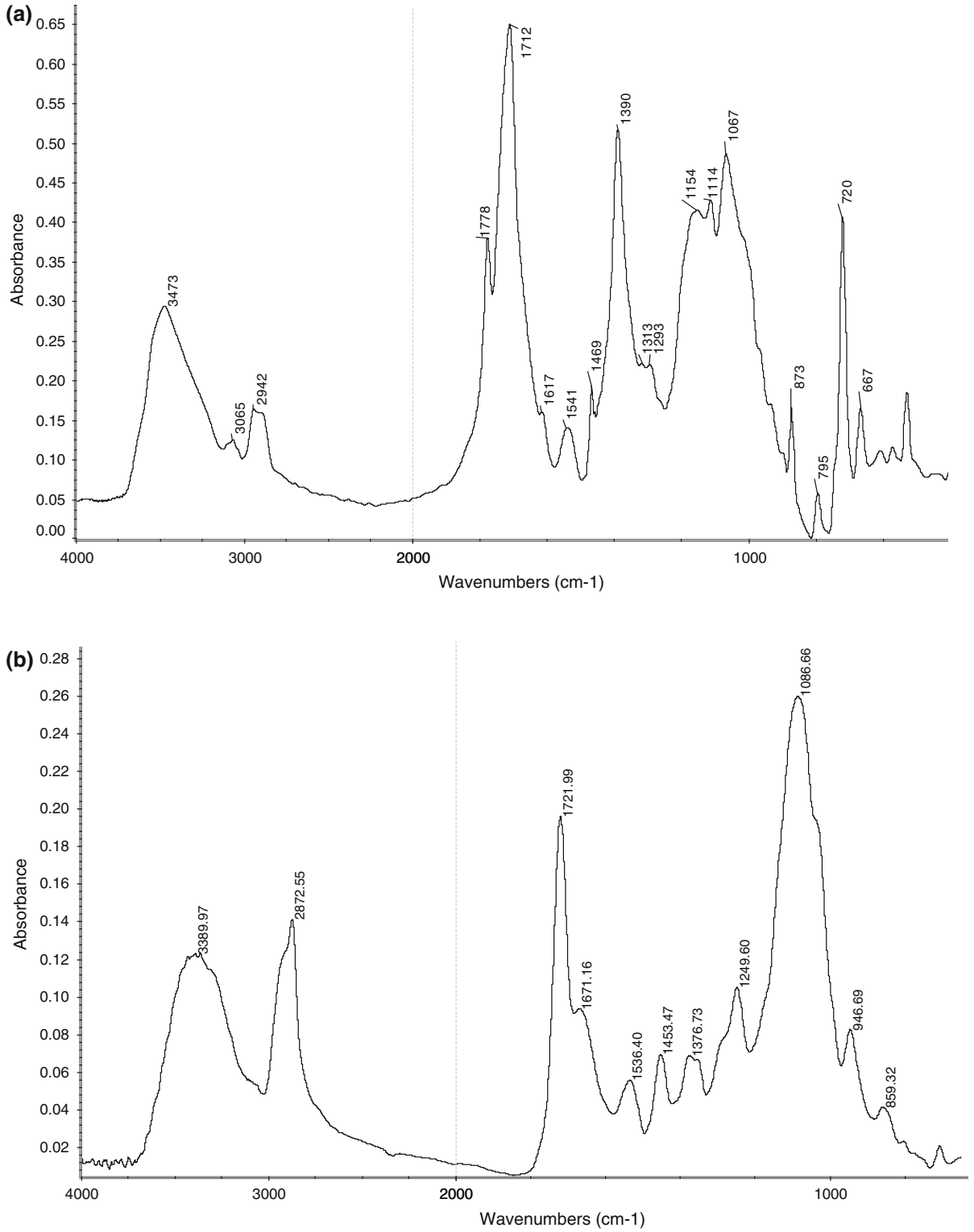

Fig. 2 FTIR spectra of **a** phthaloylated chitosan (PACS) and **b** vinyl chitosan

form the phthalimide group. The FTIR spectrum of the phthaloylated CS (PACS) as shown in Fig. 2a clearly reveals the imide absorption peaks at 1,712 and 1,778 cm^{-1}. The phenyl ring of phthalimide group was also observed at 720 cm^{-1}. From the C/N ratio of elemental analysis, the degree of phthaloylation (DS_{PA}) was calculated as 0.88 (C: 52.57 %, N: 4.58 %, H: 5.03 %). This value was slightly greater than the DDA value of original CS (DDA = 0.85), indicating the hydroxyl group in CS also reacted with PA yet with a very small extent. This *N*,*O*-phthaloylated CS could be soluble in some organic solvents such as DMF, DMAc and DMSO due to a small extent of *O*-phthaloylation. Still, a lot of hydroxyl groups remained available for further reaction. The PACS (DS_{PA} = 0.88) was then reacted with IPDI, a vinyl compound containing isocyanate group (cf. Fig. 1). Since most amino groups were protected, it was believed that the IPDI preferred to react with the remaining hydroxyl group at the C-6 position than with that at the C-3 position due to the effect of steric hindrance. A bulky phthaloyl group at the C-2 position would prevent the approaching of IPDI (also a bulky compound) to the adjacent C-3 position. After incorporating vinyl group to PACS, the phthaloyl groups for the protection of amino groups were removed by reaction with hydrazine. The characteristic absorption peaks of imide (1,778 and 1,712 cm^{-1}) and phenylene (720 cm^{-1}) in the phthaloyl group were no longer observed as shown in Fig. 2b. This indicated that most phthaloyl groups were removed by hydrazine. Though, it was possible that the hydrazine treatment also broke the carbamate linkage at C6 position that would reduce the addition extent of vinyl group. Yet, FTIR spectrum in Fig. 2b clearly shows that there was a strong absorption peak of C=O stretching of carbamate linkage at 1,718 cm^{-1}. In addition, the weak absorption peak at 698 cm^{-1} was caused by the phenylene ring of IPDI. Most importantly, the C=C double bond was still observed at 1,628 cm^{-1}, and also seen at 5.23 and 5.49 ppm in the ^{1}H NMR spectrum. These results proved the successful substitution of IPDI at C6 position even after hydrazine treatment. By using elemental analysis, the degree of addition of IPDI (DS_{IPDI}) was calculated to be 0.41 from the C/N and C/H ratios (C: 52.40 %, N: 7.42 %, H: 7.14 %).

For the crosslinking of CS, the vinyl CS was dissolved in formic acid and then added with different amounts of PEGDMA and photo initiator. Table 1 lists the recipes of the reaction systems. Upon UV irradiation, the photo initiator decomposed to free radicals and thereby PEGDMA with two double bonds was able to crosslink CS chains selectively through the vinyl group at C-6 position by a free radical polymerization as shown in Fig. 1. For comparison, a pure crosslinking PEGDMA designated as X-PEG was also synthesized via UV-initiated polymerization. Figure 3a, b shows the FTIR spectra of X-PEG and CS-*g*-PEG membranes, respectively. In the spectrum of X-PEG, a strong absorption peak at 1,724 cm^{-1} due to the C=O stretching in the ester group was observed. This ester absorption peak was also observed in the CS-*g*-PEG membranes; yet it shifted to a lower wavenumber, and the shift increased with the relative amount of CS component, indicating some interactions occurred between the CS and the PEG chains in the graft copolymer such as the hydrogen bonding between the hydroxyl and amino groups in the CS with the C=O group in the PEGDMA. Moreover, the absorption peaks at 1,658 cm^{-1} (amide I) and 1,539 cm^{-1} (amide II) in the spectrum of CS-*g*-PEG membrane were from the CS component. By a gravimetric analysis, the grafting ratio (GR) was calculated as the weight ratio of the reacted PEGDMA to the vinyl CS. The GR value not only indicated the amount of PEGDMA grafted to the CS but also the extent of crosslinking for the membrane. The conversion and grafting ratio values of CS-*g*-PEG membranes are summarized in Table 1. It can be seen that the conversion reached almost 70 % for the CS-*g*-PEG1 and then increased gradually with the feeding amount of PEGDMA. The increase in PEGDMA conversion was not only due to the increase in its concentration but also due to the decrease in the viscosity of the reaction medium, since the PEGDMA had a much lower viscosity than the vinyl CS in the formic acid solution. The same trend was found for the GR, which increased from 0.69 for the CS-*g*-PEG1 to 2.43 for the CS-*g*-PEG3. A higher GR value indicated a higher crosslinking density in the membrane. Figure 4 shows the swelling ratio of various CS-*g*-PEG membranes at 37 °C yet in two different pH buffers. Indeed, with the higher grafting ratio and crosslinking density, the swelling ratio was lower. In addition, there was no difference in the swelling ratio for the X-PEG membrane at two different pH buffers; yet, the swelling ratio was higher in a more acidic

Table 1 Conversion and grafting ratio of the prepared CS-*g*-PEG copolymer membranes, along with their C=O absorption peak from FTIR spectra

Sample	CS-*g*-PEG1	CS-*g*-PEG2	CS-*g*-PEG3
Vinyl CS (g)	0.30	0.30	0.30
PEGDMA (g)	0.30	0.60	0.90
Conversion X (%)	69	76	81
Grafting ratio	0.69	1.52	2.43
C=O (cm^{-1})[a]	1,716	1,720	1,721

[a] Pure crosslinked X-PEG membrane had a C=O absorption peak at 1,724 cm^{-1}

environment for the CS-*g*-PEG membranes. This was due to the existence of the CS component which also confirmed that there were still a lot of amino groups present along the CS chains. These amino groups would be protonated in the acidic solution ($-NH_2 + H_3O^+ \rightarrow -NH_3^+ + H_2O$) that resulted in the chain extension due to the repulsive force along the cationic CS chain. In conclusion, we have successfully crosslinked CS chains by PEGDMA selectively at the C-6 position and reserved all the amino groups at the C-2 position. It has to be mentioned that the prepared membranes had a porous structure with a uniform pore-size distribution as evidenced by SEM pictures. The average pore size was about 1 μm for the CS-*g*-PEG1 and decreased to ca. 100 nm for the CS-*g*-PEG3 due to the increasing crosslinking density (please see Supplementary Fig. 1).

Thermal properties of CS-*g*-PEG membranes

Thermal degradation behavior of various CS-*g*-PEG copolymer membranes under N_2 atmosphere was studied and discussed in the aspect of their structure as shown in Fig. 5 and their degradation temperatures are summarized in Table 2. Pure CS with a molecular weight of 96 kDa started to degrade at 296 °C (T_{onset}, degradation temperature at 5 wt% loss) and had a maximum-rate degradation temperature (T_{max}, first derivative peak temperature) at 327 °C. After the addition reaction with IPDI, the prepared vinyl CS degraded earlier with the T_{onset} at 241 °C. This was because of the decrease in the hydrogen bonding and the destruction of the crystalline structure due to addition of bulky IPDI at the C-2 position that destructed the chain regularity and increased the chain spacing as well. Still, the T_{max} remained almost the same, indicating the main chain structure was the same as the original CS. On the other hand, the pure X-PEG with a crosslinking structure degraded at higher temperatures with T_{onset} and T_{max} at 321 and 412 °C, respectively. Combining vinyl CS and PEG into a graft copolymer, it exhibited a two-stage degradation behavior, where the first- and second-stage were correspondent to the degradation of vinyl CS and grafted PEGDMA chain, respectively, as clearly observed in Fig. 5b with two differential peak temperatures. This was agreed to the structure nature of a graft copolymer. It was also found that the ratio of degradation extent of these two stages was proportional to the grafting ratio. The data in Table 2 show that because of crosslinking, the T_{onset} of the CS-*g*-PEG membrane was higher than that of the vinyl CS, and it increased with increasing the crosslinking density. Moreover, the $T_{max,1}$ values of various CS-*g*-PEG membranes, corresponding to the degradation temperature of CS component, were almost the same and about 10 °C higher than of the vinyl CS. For the degradation of the PEGDMA component in the CS-*g*-PEG membranes, the corresponding $T_{max,2}$ values were 20–25 °C greater than the T_{max} of pure X-PEG. This was because the char produced from the earlier degradation of CS component could protect the left PEGDMA component and thus increased its thermal stability to some extent. Table 2 also displays the char yield of various copolymer membranes. Pure CS had a high char yield of 37 % (residual at 800 °C), whereas the vinyl CS had a lower char yield of 28 % because it had the less thermally stable IPDI group. On the contrary, a very little char yield (0.8 %) was found for the X-PEG. For the CS-*g*-PEG membranes, the char yield thus decreased proportionally with increasing the grafting ratio.

Mechanical properties of CS-*g*-PEG membranes

Chitosan is rigid and brittle, while PEG is considered as a soft material. Table 3 summarizes the tensile and dynamic mechanical properties of the crosslinking X-PEG and CS-*g*-PEG membranes. The crosslinking X-PEG membrane had low values of ultimate tensile strength and initial modulus at 1.5 and 50 MPa, respectively; while its elongation at break was about 7.5 %. The tensile mechanical properties of pure CS could not be measured because CS was too brittle. By incorporating PEGDMA into CS via crosslinking

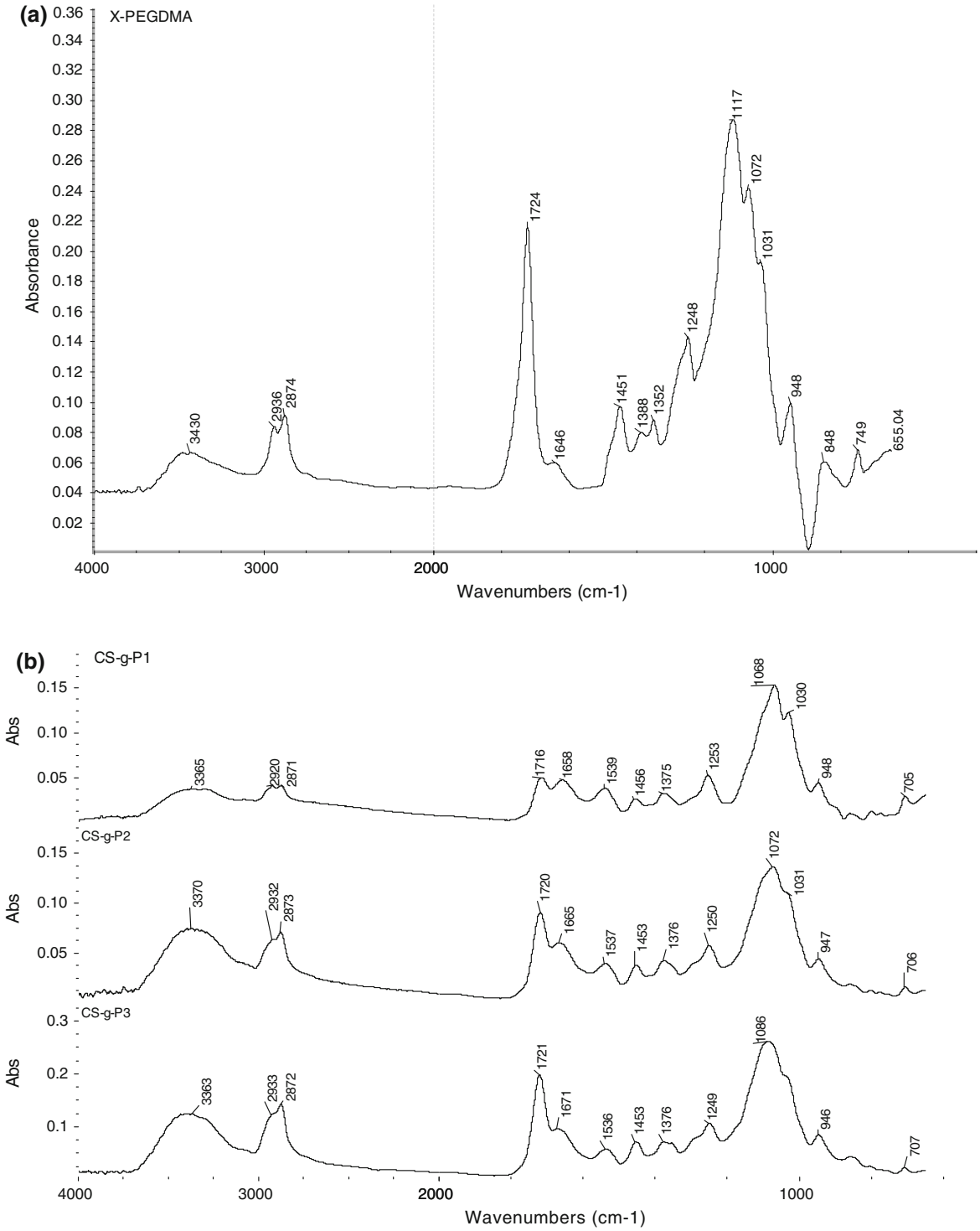

Fig. 3 FTIR spectra of **a** X-PEG membrane and **b** various CS-*g*-PEG membranes

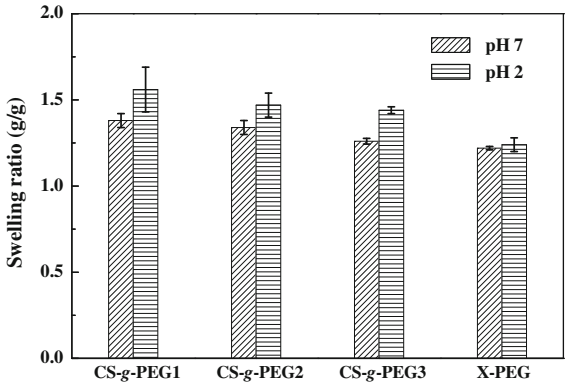

Fig. 4 Swelling ratios of the X-PEG and various CS-*g*-PEG membranes being immersed in the pH 7 and pH 2 buffer solutions both at 37 °C

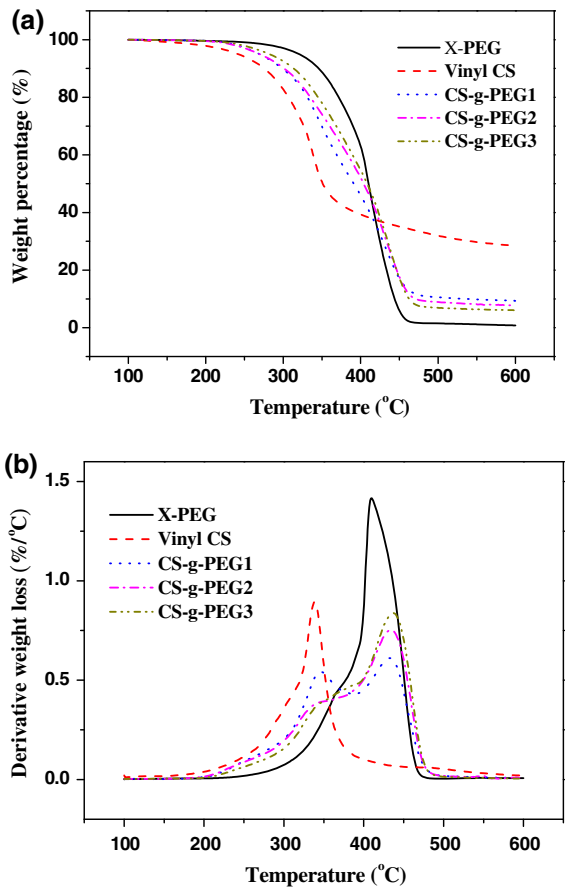

Fig. 5 **a** Weight loss curves and **b** differential weight loss curves of the X-PEG, vinyl CS and various CS-*g*-PEG membranes. The samples were heated at a heating rate of 20 °C min^{-1} under a nitrogen atmosphere

Table 2 Onset degradation temperature (T_{onset}), maximum-rate degradation temperature (T_{max})[a] and char yield of CS, vinyl CS, X-PEG and various CS-PEG membranes

Sample	CS	Vinyl CS	CS-*g*-PEG1	CS-*g*-PEG2	CS-*g*-PEG3	X-PEG
T_{onset} (°C)	296	241	269	272	281	321
T_{max1} (°C)	327	332	343	342	341	–
T_{max2} (°C)	–	–	433	434	437	412
Char yield (%)	37	28	9.4	7.7	6.1	0.8

[a] T_{onset} was the temperature at 5 % weight-loss, T_{max} was the differential peak temperature of the weight-loss curve

Table 3 Tensile mechanical properties including initial modulus (E), ultimate tensile strength (UTS) and elongation at break (ε), as well as dynamic mechanical properties including dynamic modulus E′ at 30 °C and T_g values of the X-PEG and various CS-*g*-PEG membranes

Sample	CS-*g*-PEG1	CS-*g*-PEG2	CS-*g*-PEG3	X-PEG
E (MPa)	449 ± 15	308 ± 17	197 ± 14	55.2 ± 1.0
UTS (MPa)	10.3 ± 1.3	9.9 ± 2.3	5.2 ± 0.5	1.68 ± 0.53
ε (%)	3.9 ± 1.3	4.9 ± 1.4	5.1 ± 0.6	8.0 ± 0.8
E′ (MPa)	852	527	294	24.5
$T_{g,PEG}$ (°C)	6.7	8.6	8.7	4.6
$T_{g,CS}$ (°C)	179	174	172	–

reaction, the prepared membranes were no longer brittle and had certain toughness. When CS was crosslinked by PEGDMA, actually two opposing factors could affect the mechanical properties of CS-*g*-PEG membranes. Increasing the amount of PEGDMA to crosslink CS, the material's softness would be increased due to the flexibility of PEGDMA chain itself; however, it would also increase the crosslinking density that would decrease the chain mobility. As summarized in Table 3, the results showed that both initial modulus and ultimate tensile strength of CS-*g*-PEG decreased with increasing the grafting amount of PEGDMA, while the elongation at break increased. This indicated that the flexibility of PEGDMA component surpassed the effect of crosslinking density. As a result, the incorporation of PEGDMA into CS led to the increase in toughness of material.

The variations of dynamic modulus and loss tanδ of the X-PEG and CS-*g*-PEG membranes in the dynamic mechanical analysis are shown in Fig. 6. As the

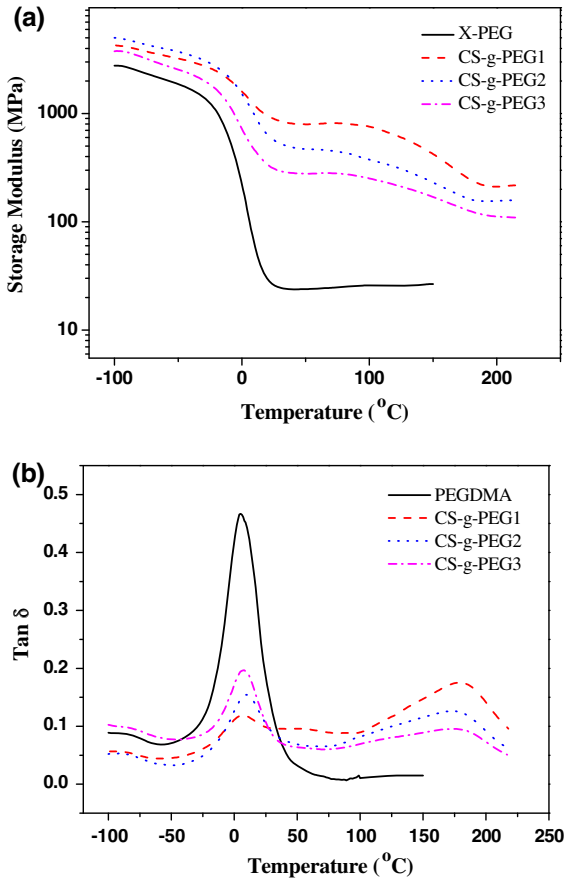

Fig. 6 **a** Storage modulus and **b** loss tanδ curves of the X-PEG and various CS-*g*-PEG membranes with temperature

temperature increased, the dynamic modulus slightly decreased until the temperature reached the material's glass transition temperature (T_g). It can be seen in Fig. 6a, there was a rapid decrease in the modulus at the T_g; For the X-PEG membrane, the decrease was about in two orders at the transition temperature about 5 °C. Above the T_g, the material was in its rubbery region. The X-PEG was thus considered as a soft elastomeric material at room temperature and its dynamic modulus at 30 °C was only 24.5 MPa. By crosslinking the PEGDMA into the CS, the material's toughness could be increased. As summarized in Table 3, the dynamic modulus decreased with increasing the grafting ratio of the PEGDMA, as the modulus at 30 °C decreased from 852 MPa for the CS-*g*-PEG1 to 294 MPa for the CS-*g*-PEG3 with the highest grafting ratio. Moreover, another rapid decrease in the modulus can be seen in Fig. 6a at higher temperature,

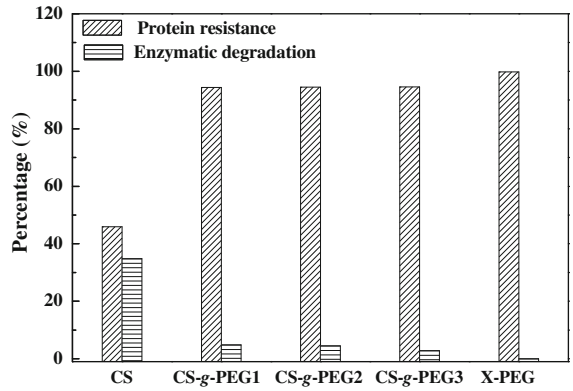

Fig. 7 Protein resistance and enzymatic degradation of CS, X-PEG and various CS-*g*-PEG membranes

which could be due to the glass transition of the CS component. This was more evident by plotting the loss tanδ curve with temperature. Figure 6b clearly reveals tow loss tanδ peaks, corresponding to the T_gs of the PEGDMA and CS chains. The T_g values are summarized in Table 3. It could be seen that the T_gs of these two components shifted to each other. This confirmed the previous argument that they had some interactions that would cause the shift of T_g. Moreover, the relative peak height ratio was proportional to the relative amount of these two components.

Protein resistance and enzymatic degradation of the CS-*g*-PEG membranes

In some biomedical applications, blood compatibility is very important especially when the material is in contact with the blood. It is known that the CS can easily cause the blood coagulation and hemostasis; yet the PEG is blood compatible and can protect the activities of enzymes. In this study, β-glucosidase was used as a model protein to test the protein resistance of the synthesized CS-*g*-PEG membranes. β-glucosidase is an enzyme that can act upon β-1,4 linkage of two glucose or glucose-substituted molecules. It is an exocellulase that catalyzes the hydrolysis of terminal non-reducing residues in β-D-glucosides with release of glucose. It has been reported that β-glucosidase can be well-immobilized onto CS and its derivatives with a yield of 60–75 % (Chang et al. 2008, 2013; Zheng et al. 2013). For the pure CS, Fig. 7 shows that after incubation with β-glucosidase for 24 h, the β-glucosidase left in solution had a residual activity of 0.17 Unit. Compared to the original enzyme solution before

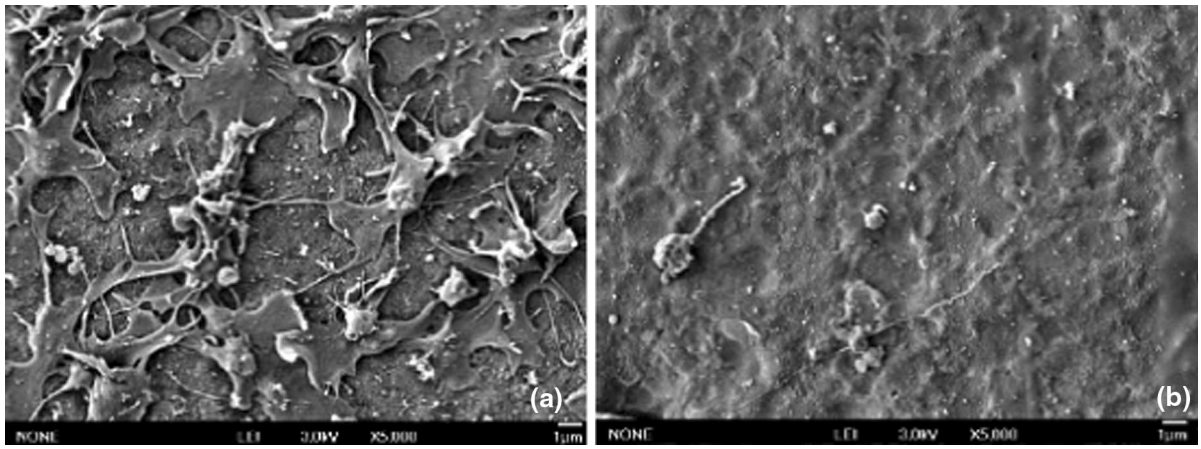

Fig. 8 Platelet adhesion on **a** chitosan membrane (*left*, ×5,000) and **b** CS-*g*-PEG2 membrane (*right*, ×5,000)

incubation which had an activity of 0.37 Unit, the immobilization efficiency was about 54.1 %. In other words, the protein resistance was 45.9 %. On the other hand, the X-PEG had an excellent protein resistance at a value of 99.8 %. Nearly no protein could be adsorbed onto the X-PEG membrane. After incorporation with the PEGDMA into the CS, it can be seen in Fig. 7 that all CS-*g*-PEG membranes had protein resistance higher than 94 %.

The enzymatic degradation was also studied by using lysozyme. It is well known that the lysozyme can degrade CS material. After incubating the pure CS with lysozyme in a pH 7.4 buffer solution at 37 °C for 2 weeks, the weight loss was found to reach 34.8 wt% as shown in Fig. 7. However, by crosslinking the CS with PEGDMA to form CS-*g*-PEG membranes, the enzymatic degradation was greatly decreased to a value less than 5 %. This was because of the crosslinking that would retard the degradation of the CS. More importantly, the PEGDMA would inhibit the protein adsorption onto the membrane. In addition, the extent of degradation decreased with increasing the grafting ratio of the PEGDMA. For the CS-*g*-PEG3 with a grafting ratio of 2.43, the enzymatic degradation was only 2.8 % after 2 weeks.

Generally, those materials which provide a suitable environment for cell growth and proliferation can also easily induce surface thrombosis. For example, CS is cellular compatible but also is highly thrombogenic due to its cationic surface charge (Amiji 1995). The extent of platelet adhesion and surface-induced activation is considered an early indication of the thrombogenic potential of blood-contacting materials. When in contact with membrane's surface, platelets initially maintain their discoid shape in the resting state. Upon activation, platelets extend their pseudopods and initiate the release of granular contents. In this study, preliminary blood compatibility was carried out by observing the surface of membranes being contacted with platelet rich plasma (PRP) for 1 h. The number of the adhered platelets was in accordance with the blood compatibility of the membrane. Figure 8a clearly reveals that platelets could adhere on the CS membrane very well with extended pseudopods. However, for the CS-*g*-PEG membranes, the number of adhering platelets was much lower as could be seen on the representative CS-*g*-PEG2 membrane as shown in Fig. 8b. The other two CS-*g*-PEG membranes had similar behavior. Suppression of platelet adhesion could be elucidated by a reduction of protein adsorption due the presence of the PEGDMA component in line with the highly protein resistance as discussed previously. This proves that the crosslinking of CS with the PEGDMA could inhibit the adhesion of platelet and thus greatly increase the blood compatibility of membrane which is beneficial for the application in hemodialysis.

Conclusions

In this study, CS was first endowed with vinyl functional group at its C-6 position via a protection-grafting-deprotection procedure. Subsequently, the

crosslinking of vinyl CS was carried out by reaction with PEGDMA through its vinyl group at the C-6 position via a UV-initiated free-radical polymerization to form CS-*g*-PEG copolymer membranes. Most active amino groups at the C-2 position of CS pyranose were reserved in the CS-*g*-PEG membranes. FTIR and NMR analyses confirmed the structures of the prepared CS-*g*-PEG copolymer membranes. In addition, some interactions occurred between the CS main chain and the grafted PEGDMA chain that the glass transition temperatures of the CS and PEGDMA component shifted to each other. The incorporation of the PEGDMA increased the material's flexibility and thermal resistance. In addition, the CS-*g*-PEG membranes were found to have good protein resistance and blood compatibility; therefore, it has potential application as the biomedical material especially for hemodialysis.

Acknowledgments The authors wish to express their appreciation for the financial support from the National Science Council in Taiwan. The authors also want to thank Ms. Ching-Wei Lu in National Taiwan University for the help on the elemental analysis.

References

Amiji MM (1995) Permeability and blood compatibility properties of chitosan-poly(ethylene oxide) blend membranes for haemodialysis. Biomaterials 16(8):593–599

Bhattarai N, Ramay HR, Gunn J, Matsen FA, Zhang M (2005) PEG-grafted chitosan as an injectable thermosensitive hydrogel for sustained protein release. J Control Release 103:609–624

Chang MY, Kao HC, Juang RS (2008) Thermal inactivation and reactivity of β-glucosidase immobilized on chitosan-clay composite. Int J Biol Macromol 43(1):48–53

Chang J, Lee YS, Fang SJ, Park DJ, Choi YL (2013) Hydrolysis of isoflavone glycoside by immobilization of β-glucosidase on a chitosan-carbon in two-phase system. Int J Biol Macromol 61:465–470

Colonna C, Conti B, Perugini P, Pavanetto F, Modena T, Dorati R, Iadarola P, Genta I (2008) Site-directed PEGylation as successful approach to improve the enzyme replacement in the case of prolidase. Int J Pharm 358:230–237

Don TM, Chen HR (2005) Synthesis and characterization of AB-crosslinked graft copolymers based on maleilated chitosan and N-isopropylacrylamide. Carbohydr Polym 61(3):334–347

Don TM, Chou SC, Cheng LP, Tai HY (2011) Cellular compatibility of copolymer hydrogels based on site-selectively-modified chitosan with poly(N-isopropyl acrylamide). J Appl Polym Sci 120(1):1–12

Harish Prashanth KV, Tharanathan RN (2007) Chitin/chitosan: modifications and their unlimited application potential- an overview. Trends Food Sci Technol 18:117–131

Lavertu M, Xia Z, Serreqi AN, Berrada M, Rodrigues A, Wang D, Buschmann MD, Gupta AA (2003) Validated 1H NMR method for the determination of the degree of deacetylation of chitosan. J Pharm Biomed Anal 32(6):1149–1158

Li Q, Yang D, Ma G, Xu Q, Chen X, Lu F, Nie J (2009) Synthesis and characterization of chitosan-based hydrogels. Int J Biol Macromol 44:121–127

Lin WJ, Chen MH (2007) Synthesis of multifunctional chitosan with galactose as a targeting ligand for glycoprotein receptor. Carbohydr Polym 67(4):474–480

Mao S, Germershaus O, Fischer D, Linn T, Schnepf R, Kissel T (2005) Uptake and transport of PEG-graft-trimethyl-chitosan copolymer–insulin nanocomplexes by epithelial cells. Pharm Res 22:2058–2068

Peng H, Xiong H, Li J, Chen L, Zhao Q (2010) Methoxy poly(ethylene glycol)-grafted-chitosan based microcapsules: synthesis, characterization and properties as a potential hydrophilic wall material for stabilization and controlled release of algal oil. J Food Eng 101:113–119

Radhakumary C, Nair PD, Nair CPR, Mathew S (2009) Chitosan-*comb-graft*-polyethylene glycol monomethacrylate: synthesis, characterization, and evaluation as a biomaterial for hemodialysis applications. J Appl Polym Sci 114(5):2873–2886

Rinaudo M (2006) Chitin and chitosan: properties and applications. Prog Polym Sci 31:603–632

Zheng P, Wang J, Lu C, Xu Y, Sun Z (2013) Immobilized β-glucosidase on magnetic chitosan microspheres for hydrolysis of straw cellulose. Process Biochem 48(4):683–687